Boosting the Bounds of Symbolic QED for Effective Pre-Silicon Verification of Processor Cores

Karthik Ganesan, *Student Member*, Srinivasa Shashank Nuthakki, *Student Member*

***Abstract*— Existing techniques to ensure functional correctness and hardware trust during pre-silicon verification face severe limitations. In this work, we systematically leverage two key ideas: 1) Symbolic QED, a recent bug detection and localization technique using Bounded Model Checking (BMC); and 2) Symbolic starting states, to present a method that: i) Effectively detects both "difficult" logic bugs and Hardware Trojans, even with long activation sequences where traditional BMC techniques fail; and ii) Does not need skilled manual guidance for writing test-benches, writing design-specific assertions, or debugging spurious counter-examples. Using open-source RISC-V cores, we demonstrate the following: 1. Quick (≤5 minutes for an in-order scalar core and ≤2.5 hours for an out-of-order superscalar core) detection of 100% of hundreds of logic bug and hardware Trojan scenarios from commercial chips and research literature, and 97.9% of "extremal" bugs (randomly-generated bugs requiring ~100,000 activation instructions taken from random test programs). 2. Quick (~1 minute) detection of several previously unknown bugs in open-source RISC-V designs.**

***Index Terms* — Formal Verification, Symbolic Quick Error Detection, Hardware Trojans, Pre-silicon Verification, Bounded Model Checking.**

I. Introduction

Pre-silicon verification requires major effort in a typical hardware design flow [1]. In this paper, we consider pre-silicon verification of single processor cores, which are critical components of any System-on-Chip (*SoC*). Generally, pre-silicon verification mainly targets logic design errors (*logic bugs*). However, it is also crucial to detect Hardware Trojans (*HTs*) [2], which are unauthorized modification of a system that result in incorrect functionality and/or the exposure of sensitive data [3]. While previous research on HTs focused on attacks implemented during fabrication [4], there is growing concern about HTs being inserted in third-party Intellectual Property (*IP*) cores by malicious entities [5]. This makes HT detection during pre-silicon verification essential.

Similar to logic bugs, HTs can affect functionality of a system. For example, an HT can cause an error that creates a change in the software-visible state of a system, defined by the state of software-visible registers and memory. The objective of HT detection is to detect these changes, which encompass many catastrophic attacks on processor cores [2].

Symbolic quick error detection (*Symbolic QED* or *SQED*) [6] is a new pre-silicon verification technique based on QED tests [7]. It uses bounded model checking (*BMC*) [8] for formal analysis of the design. QED tests generate short sequences of instructions that trigger logic bugs in a design. As such, SQED is an automatic bug detection and localization technique that is extremely effective in practice.

Manuscript received Aug. 15, 2019. K. Ganesan and S. S. Nuthakki are with Dept. of Electrical Engineering, Stanford University, Stanford, CA 94305 USA (e-mail: karthik3@stanford.edu). An early draft is cited in [9] as [Ganesan 18].

For example, SQED was recently applied to several industrial microcontroller cores used in commercial automotive products [9]. It was able to detect all recorded logic bugs in the designs, while enabling an 8-60X (depending on the design) reduction in verification effort compared to the standard industrial verification flow.

Importantly, SQED does not target single-instruction bugs (i.e., bugs such that a single instruction on a specific set of inputs always produces an incorrect result). There are many other verification techniques that are highly effective at detecting such bugs, from both research literature [10] and in industry [9].

SQED analyzes a design symbolically, but it requires a *concrete* starting state (e.g., a state of the digital system that is given explicitly as a bit-vector of 0s and 1s). That means, to find bugs or HTs that require long activation sequences (i.e., many instructions are required to activate such bugs), Symbolic QED must rely on very deep BMC runs (i.e., runs that unroll the system far enough to include all the activation instructions). This can be very difficult for practical designs. In a related study [6], it was shown that BMC could unroll a large, multicore SoC up to around 30 clock cycles, within 24 hours of verification time. The following example [11] shows that SQED, while highly effective for logic bugs, can be insufficient for detecting HTs.

Motivating Example 1. Consider the following HT that is difficult to find using existing HT detection techniques: *The HT changes opcodes of the next several decoded instructions if the processor has fetched a specific sequence of 256 instructions.* This HT could inject an instruction sequence to bypass physical memory protection and run a privileged instruction. Such privilege escalation attacks [2] can be catastrophic.

Because the HT requires a long sequence of instructions (and hence many clock cycles) for activation, SQED (like other BMC-based methods [12, 13]) fails to detect the HT unless the selected starting state for BMC quickly transitions to a state where the HT activates. Stumbling upon such a "close" state by starting at a concrete state (e.g., obtained from simulation or a power-on reset state) is highly unlikely to succeed since the HT can be designed with an arbitrary activation sequence that is not known *a priori*.

To overcome this major challenge, we extend SQED so that it is now capable of starting from a *symbolic* (instead of concrete) starting state (i.e., we give the BMC tool the ability to choose an arbitrary starting state for each run).

However, it is well-known that starting BMC from an unrestricted symbolic starting state risks generating *spurious counterexamples* (*false positives*). This occurs when the BMC tool incorrectly indicates that a bug or HT is present in a design, when there is actually no bug or HT. If the BMC tool selects a starting state that is not reachable from the set of all reset states of the system via a sequence of instructions, then a false positive

might occur. For example, assume that each word in a memory system is protected with a single even parity bit and assume that a BMC tool is asked to check the following property: *for any sequence of reads and writes to the memory, the parity bits remain consistent with the data.* If the starting state of the design is not constrained, then the BMC tool can initialize the memory to contain an all-zero word with a '1' for the parity bit, issue an instruction that reads from this location, check the property, and report this false positive.

Traditional methods rely on verification engineers to (manually) create constraints to rule out such false positives, which can be time-consuming for practical designs having many complex properties. This paper overcomes that challenge by: i) defining *QED constraints*: sufficient constraints (see Section III for details and Appendix B for proofs) to ensure false positives do not occur when using Symbolic QED with symbolic starting states; and ii) introducing *QED recorders*, which observe a small subset of internal signals within the processor to ensure the QED constraints are satisfied. QED recorders are used for pre-silicon verification only. They do not incur area overhead for the final design.

Our work improves on a previous technique for SQED with symbolic initial states, called S^{2}QED [14]. That approach differs from ours in the types of processors that can be verified, the types of logic bugs and HTs that can be detected, and the way symbolic initial states are implemented. We explain our advantages in Section II.C.

Experimental results using our new method demonstrate:

1. We automatically, correctly, and quickly (~1 minute) detect several previously unknown (real) logic bugs in open-source out-of-order (OoO) superscalar [15], and in-order scalar [16] RISC-V cores. The bugs found in [15] cannot be detected by [6] or [14].
2. We automatically, correctly, and quickly (within 25 seconds for in-order, 18 minutes for OoO) detect 100% of (117 in-order, 120 OoO) simulated logic bugs, representing a wide variety of "difficult" logic bugs (Appendix A) from commercial designs. SQED with a concrete starting state detects only 33% (in-order) and 5% (OoO).
3. We automatically, correctly, and quickly (within 5 minutes for an in-order core; 2 hours for an OoO superscalar core) detected 100% of (156 in-order, 195 OoO) simulated HTs, encompassing a wide variety of scenarios (Appendix A) from over 100 papers in the HT research literature. SQED with a concrete starting state detects 15% (in-order) and 9% (OoO).
4. We automatically, correctly, and quickly (within 2.5 hours) detected 97.9% of an "extremal" bug family (randomly-generated pre-condition-based bugs which require ~100,000 activation instructions taken from random test programs) in an OoO superscalar core [15]. In contrast, SQED with a concrete starting state detected 0%, and [14] is not applicable.

Important features of our new technique are:

1. It is highly effective for detecting both logic bugs and HTs (despite long activation sequences) during pre-silicon verification of in-order and OoO superscalar cores, as demonstrated by our results.
2. It does not require the verification engineer to manually craft design-specific assertions to detect logic bugs or HTs.
3. No false positives occurred, as demonstrated by our results.
4. It does not require a golden model or simulation data of the design-under-test for detection of logic bugs and/or HTs.
5. Its effectiveness does not depend on the way HTs are designed, i.e., our method is HT-design agnostic.

The rest of this paper is organized as follows. Section II provides background on earlier QED works. Section III describes Symbolic QED with symbolic starting states. Results are presented in Section IV, followed by a survey of related work in Section V and conclusions in Section VI.

Appendix A provides a list of logic bug and HT types used in the experiments of Section IV. Appendix B provides formal proofs of the sufficiency of QED constraints (introduced in Section III.B). Appendix C provides details on how QED constraints are specified to the BMC tool.

II. Background

In the following, we present the basics and terminology of QED [7], SQED [6], and S^{2}QED [14].

A. QED and the EDDI-V Transformation

Quick error detection (*QED*) is a testing technique that takes existing system validation tests (i.e., sequences of instructions) and automatically transforms them into a set of new tests using various QED transformations [7]. Among the various transformations that can be applied, Error Detection using Duplicated Instructions for Validation (*EDDI-V*) is the focus of our work (illustrated in Fig. 1). It targets bugs inside processor cores by checking the results of *original* instructions against the results of *duplicate* instructions.

First, the software-visible register and memory space are divided into two halves, one for the original instructions and one for the duplicated instructions. Next, corresponding registers and memory locations for the original and duplicated instructions are initialized to hold the same values. This is called a *QED-consistent* system state. Then, for every load, store, arithmetic, logical, shift, or move instruction in the original test, EDDI-V creates a corresponding duplicate instruction that performs the same operation, but uses only registers and memory reserved for the duplicate ones. The duplicated instructions execute after the original instructions (in the same relative order), but may be interleaved. The EDDI-V transformation then inserts periodic check instructions that compare the results of the original instructions against those of the duplicated ones. A failing QED test occurs if after an equal number of original and duplicate instructions have committed, the system reaches a state that is not QED-consistent. The respective starting state and instruction sequence constitute a *counterexample* or *QED-compatible* bug trace.

```
R1 = R1 + 5
R3 = R1 * R2
```
a)

```
R1 = R1 + 5
R3 = R1 * R2
R17 = R17 + 5
R19 = R17 * R18
```
b)

Fig. 1. Example of EDDI-V transformation. a) A sequence of original instructions; b) Transformed instructions executed by the processor. R17, R18, and R19 are the duplicate registers of R1, R2, and R3 respectively.

B. Symbolic QED

Symbolic QED [6] combines QED transformations with bounded model checking [8, 17] for pre-silicon verification of a design. SQED creates a BMC problem to check *all possible* EDDI-V tests within a bounded number of clock cycles for a

failing one. It searches for counterexamples to properties of the form $\mathrm{Ra} == \mathrm{Ra}'$. Here, Ra is an original register, and Ra' is the corresponding duplicate register in an EDDI-V test. To ensure that all possible counterexamples are QED-compatible: 1. Original instructions must be valid instructions from the instruction set architecture (*ISA*) of the design; 2. The instruction sequence must be an EDDI-V test.

A *QED module* (a small hardware module that is only used during pre-silicon verification and does not incur area overhead for the final design) automatically transforms a sequence of original instructions into a QED-compatible sequence (e.g., as in Fig. 1). The QED module only requires that the input sequence is made up of valid instructions that read or write to only the original registers and memory (conditions that can be specified directly to the BMC tool). After execution, a signal is asserted (denoted below as $\mathrm{QED}_{\mathrm{ready}}$). All original and corresponding duplicate registers should contain the same values in a bug-free situation, i.e., the BMC tool checks that

$$\uparrow(\mathrm{QED}_{\mathrm{ready}}) \Rightarrow \bigwedge_{a \in \{1,\ldots,\frac{N}{2}\}} \mathrm{Ra} == \mathrm{Ra}'$$

where N is the number of registers defined by the ISA. Here (for $a \in \{1, \ldots, N/2\}$), Ra and Ra' correspond to original and duplicate registers. $\uparrow(\mathrm{QED}_{\mathrm{ready}})$ is true on any clock edge where $\mathrm{QED}_{\mathrm{ready}}$ transitions from low to high.

The starting state for the BMC run must also be a QED-consistent state, in which the value stored in each original register or memory location matches the corresponding duplicate register or memory location. This is to prevent spurious counterexamples from being generated. One way to obtain such a state is to run an EDDI-V test in simulation and stop immediately after QED checks have compared all register and memory values.

Symbolic QED can also detect HTs, if it finds an EDDI-V test for which the HT affects original registers and duplicate registers differently. For example, assume an HT is inserted (unknown to the designer) that activates when a 128-bit counter reaches its maximum value. Assume the HT changes an in-flight instruction to a NOP when it activates (cf., activation criteria A.2.a.2 ($X_1 = 128$) of Appendix A and effect A.2.b.1 of Appendix A). If the counter is initialized to the value $2^{128} - 1$, and the register file is initialized in a QED-consistent state, SQED can detect the HT using the EDDI-V test {ADDI R1, R1, 2; ADDI R17, R17, 2; CHECK R1==R17}. However, as the existence of the counter is unknown, it is impossible to pick the proper concrete starting state *a priori*. Instead, our approach to SQED with symbolic starting states (detailed in Section III) automatically detects this HT by starting the design at a state where $\{\mathrm{Counter} = 2^{128} - 1;\ \mathrm{R1}{=}0;\ \mathrm{R17}{=}0\}$ and running the above EDDI-V test.

C. S^2QED

S^2QED [14] is another technique for pre-silicon verification of processor cores which extends SQED by incorporating symbolic initial states. Like the approach in this paper, S^2QED focuses only on EDDI-V tests. S^2QED instantiates two copies of the CPU-under-test, called CPU-1 and CPU-2. An arbitrary bijective mapping is then determined between the general-purpose registers and memory locations of the two CPU instances. A new notion of "QED-consistency" (which we refer to as *S^2QED-consistency*) is achieved by any state where all values in the general- and special-purpose registers and memory locations of CPU-1 match the values in the mapped registers and memory locations of CPU-2.

At the start of verification, both CPUs are initialized to a S^2QED-consistent state. CPU-1 fetches an instruction called the instruction under verification (IUV) while CPU-2 fetches the corresponding S^2QED duplicate instruction (i.e., the same instruction but with operand specifiers replaced by corresponding register or memory locations for CPU-2). In the following clock cycles, CPU-1 is constrained to fetch NOPs until the IUV commits, while CPU-2 can fetch arbitrary valid instructions (treated as symbolic instructions by the BMC tool). S^2QED then attempts to prove that directly after the IUV and its S^2QED duplicate commit, the CPUs remain S^2QED-consistent. Thus, S^2QED is can prove that the model of the processor design is free of bugs of a specific type.

However, S^2QED [14] is unable to detect a (large) class of logic bugs and HTs that SQED [6] and the new method in this paper are able to detect:

Motivating Example 2. *When all registers in the general-purpose register file contain the same value, a logic bug or HT attack is triggered.*

These bugs and HTs escape S^2QED, because they affect the original and duplicate CPU equivalently. In contrast, our new approach detects the bugs and HTs by creating scenarios where mismatches between original and duplicate instructions occur.

To count how many distinct logic bugs and HTs could exist from the above class, the benchmark core [18] used in [14] has 16 distinct 32-bit general-purpose registers. There are at least 2^{32} distinct logic bug activation types (Appendix A; Table A.1.a.3 with R=16) and at least 2^{32} distinct HT activation scenarios (Appendix A; Table A.2.a.3 with M_2=16) which fall under Motivating Example 2 that are considered in our experiments in Section IV. Multiplying this by at least 3 distinct logic bug effects (Appendix A; Table A.1.b.1-3) and at least 4 distinct HT effects (Appendix A; Table A.2.b.1-4), there are at least 12 billion distinct logic bugs and at least 17 billion distinct HTs that would not be caught by S^2QED, but will be caught by our new technique.

Our approach also differs from S^2QED in that it is especially suited for a broader class of processor designs, including OoO superscalar processors. This capability is enabled by the QED constraints we define (Section III.B), together with QED recorders (Section III.C) and a new QED module (Section III.C). In contrast to our approach, S^2QED is applicable to processors with Out-of-Order writeback. This is possible due to additional constraints that restrict the state of the instruction pipeline. Such constraints can also be integrated in our framework. Further, S^2QED does not require a QED module or QED recorders. However, it requires duplication of the CPU in the model of the design-under-test (only during pre-silicon verification), whereas our approach requires only a single CPU.

III. Extending SQED with Symbolic Starting States

We now present our new extension of SQED [6] with symbolic starting states. In Section III.A, we describe the design of a new, improved QED module that is integrated in the model of the design-under-test during pre-silicon verification. These improvements enable the detection of real logic bugs that

[6] fails to detect (see Section IV.A). Section III.B introduces a set of QED-constraints on the symbolic starting state that allow us to avoid false positives. The sufficiency of these constraints is proven in Appendix B. To implement the QED-constraints, we introduce QED-recorders in Section III.C. These are additional hardware modules (used only during pre-silicon verification) that record a small subset of internal logic values of the processor core to ensure that the QED-constraints are satisfied when a QED test begins. Fig. 2 contrasts Symbolic QED without/with symbolic starting states.

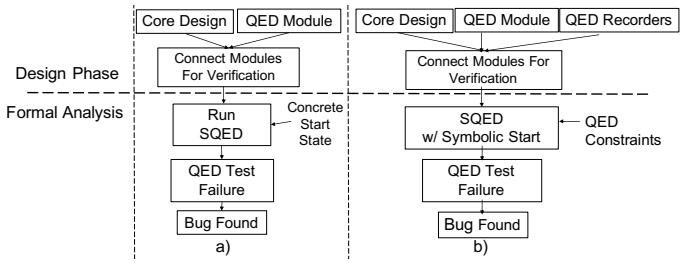

Fig. 2. Symbolic QED without/with symbolic starting states. a) SQED inputs and steps with concrete starting state; b) SQED inputs and steps with symbolic starting state.

A. New QED Module for Single Processor Cores

Pseudocode for the new QED module is given in Fig. 3a. Inputs are: 1) *enable*: disables the QED module if false; 2) *next_instruction*: next instruction to be executed; 3) *fetch_next*: true when the core is ready to receive an instruction, i.e., the fetch stage is not stalled; 4) *original*: tells the core to execute an original (if true) or duplicate (if false) instruction. Outputs are: 1) *instruction_valid*: indicates whether the output instruction is valid; and 2) *instruction_out*: instruction to be executed. The QED module has internal variables: 1) *queue*: a queue data structure that stores previous original instructions that have not yet been executed in the duplicate subsequence; 2) *head_instruction*: the previous head of the queue; 3) *insert_valid*: true when an instruction is loaded into the queue; 4) *delete_valid*: true when the QED module can execute a duplicate instruction; 5) *duplicate_instruction*: next instruction in duplicate subsequence to execute (when *original* is false).

QED checks occur when the *qed_ready* signal of the QED module is true. Pseudocode for determining this signal is given in Fig. 3b. To avoid trivial false positives, QED checks occur when an equal number of commits (writes) have been made to original registers and duplicate registers. This is accomplished by keeping track of the number of original and duplicate commits to the register set, as shown in Fig. 3b. For simplicity, in Fig. 3b, we assume that at most one instruction commits per cycle. For superscalar processors that can commit multiple instructions in the same cycle, we track all corresponding pairs of *write_valid* (tells whether the input data is valid) and *write_address* (the address for the data to be written) signals, keep a separate *is_original* signal (identifies if a write address corresponds to an original or duplicate location) for each instruction, and allow the original and duplicate counters to be incremented multiple times if needed.

The old QED module of [6] requires that all original instructions complete, a waiting period occurs for the pipeline to be flushed, and duplicate instructions execute, before the qed_ready signal is asserted. In constrast, this new QED module allows arbitrary interleaving of the original and duplicate instruction subsequences, without requiring a waiting period. This additional timing diversity is made possible by giving the BMC tool control over the *original* input of Fig. 3a. The QED-ready logic (Fig. 3b) can be further enhanced as follows:

1. The current QED-ready logic is only applicable to single processor cores, since a multi-core system would require considering the original and duplicate commits across all cores. This can be challenging in situations where multiple cores operate with a shared address space. For simplicity, we do not consider this situation in this paper.
2. For some processors, e.g., superscalar processors with explicit register renaming (MIPS 10000 [19] and ARM's Cortex-A15 [20]), the designation of original or duplicate instruction cannot be made solely on physical address (unlike in Fig. 3b). This issue can be corrected by including the current state of the register mapping table as an input to the function is_write_to_original_space. Each time a QED check happens, the same mapping table must be used to map logical to physical addresses before comparing original and duplicate values. The RISC-V cores used in our experimental evaluation (see Section IV), however, do not have this issue.

```
INPUT: enable, next_instruction, fetch_next, original
OUTPUT: instruction_out, instruction_valid
// initialization
queue ← 0;  head_instruction ← 0;
// end initialization
insert_valid  ← fetch_next & original & ~queue.is_full();
delete_valid ← fetch_next & ~original & ~queue.is_empty();
instruction_valid ← insert_valid | delete_valid;
if insert_valid then
  queue.push(next_instruction);   // store next instruction in queue
else if delete_valid then
  head_inst ← queue.pop();        // remove head instruction
end if
duplicate_instruction←create_duplicated_version(head_inst);
instruction_out ← (enable & ~original) ?
                        duplicate_instruction : next_instruction;
```

a)

```
INPUT: write_valid, write_address
OUTPUT: qed_ready
// initialization
qed_ready ← false; count_original ← 0; count_duplicate ← 0;
// end initialization
is_original ( is_write_to_original_space(write_address);
if write_valid then
  if is_original then
    count_original++;    // increment num. orig. insts. committed
  else
    count_duplicate++; // increment num. dup. insts. committed
  end if
end if
qed_ready ← (count_original == count_duplicate) ? true : false;
```

b)

Fig. 3. Pseudocode for a) New QED module; b) QED-ready enable logic.

B. QED Constraints

We first define some terminology used in the constraint definitions: i) Symbolic In-Flight (SIF) "instructions": symbols (i.e., state bits), part of the symbolic starting state (which will be assigned 0s and 1s by the BMC tool), corresponding to (microarchitectural) flip-flops within the pipeline that hold

instructions during normal operation of the core[1]; ii) T_C: the point in time when all SIF instructions have committed (i.e., written to the architectural state). This is determined by the BMC tool. iii) *Symbolic QED instructions*: symbols which represent the instructions that form the bug trace (which is part of the counterexample, along with the starting state that BMC assigns) generated by the BMC tool after T_C; and iv) *Symbolic QED operand data*: symbols representing the operand[2] data of dispatched Symbolic QED instructions (dispatched before T_C).

Fig. 4 illustrates these definitions for a 3-stage in-order pipeline. When the formal analysis begins, there are up to 3 SIF instructions in the pipeline, and all commit by time T_C. The first Symbolic QED instruction (R1=R1+5 in Cycle 1 of Fig. 4) is fetched into the pipeline, and its Symbolic QED operand data is available after the Dispatch stage.

Now, the QED constraints are stated as follows (Appendix C further details how each constraint is enforced):

Constraint C-1. At T_C, all SIF instructions have committed (i.e., no SIF instruction can write to the architectural state after T_C), while all Symbolic QED instructions commit after T_C.

Constraint C-2. At T_C, the architectural state (program-visible registers and memory) is QED-consistent (Section II.B), and nothing but Symbolic QED instructions can write to architectural state after T_C (e.g., test modes such as scan that bypass instructions to write to architectural state are disabled).

Constraint C-3. All the operand data for each Symbolic QED instruction *I*, must satisfy one of the following properties:

i) if operand data is available (i.e., *I* has already read data for this operand) at T_C then it matches the corresponding register or memory location (i.e., source operand location) data at T_C.

ii)[3] if operand data is not available at T_C, then *I* is waiting for the result of an earlier Symbolic QED instruction for this operand data.

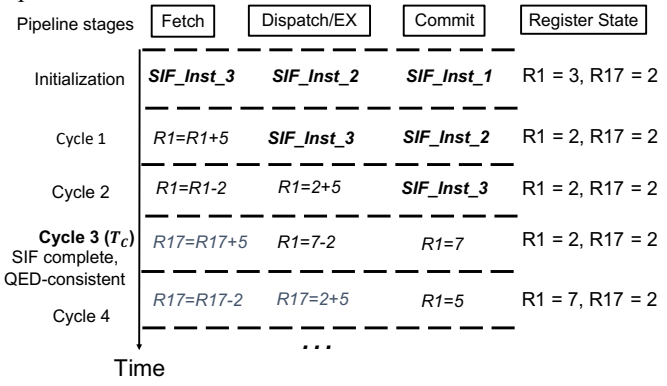

Fig. 4. Timing diagram for a three-stage in-order pipeline satisfying all QED constraints. SIF instructions commit by time T_C, before all SQED instructions.

The QED constraints form a sufficient condition to ensure no false positives, given that bug-free designs satisfy two assumptions after T_C:

Assumption-1. If a Symbolic QED instruction is executed twice on the same data, it results in the same value being stored to architectural state, e.g., Rx=1+2; and Ry=1+2 always result in the same value stored to both registers Rx, and Ry. Note: there is no assumption that the stored value is '3'.

Assumption-2. If a Symbolic QED instruction has a read-after-write dependency with earlier instructions, it uses the most recent value of the data in its computation. For example, in the program {R1=5; R2=R1+2; R3=R2-2}, if the first instruction stored '5' to architectural-state, the second instruction will use value '5' for R1.

We can now state the main theorem of the paper. Formal definitions and full proofs are deferred to Appendix B.

Theorem 1. Let Constraints C-1, C-2, and C-3 be satisfied by a starting state of a processor core. Let *Assumptions-1 and -2* hold after T_C for any bug-free design of the core. If any EDDI-V test fails, the failure must be caused by a bug in the design.

Proof: See Appendix B. ■

PROOF OUTLINE: We first define notation for a sequence of Symbolic QED instructions in a QED-compatible bug trace. Next, we isolate the first pair of Symbolic QED instructions which cause an EDDI-V test failure. We decompose the execution of these two instructions into a union of six mutually disjoint cases. For each case, we give a proof by contradiction (of one or more *Assumptions*) that there must be a bug in the design, thus concluding the proof. ■

We also observed empirically (see Section IV), that at least one assumption was violated in each BMC bug trace.

C. Symbolic QED Recorders

QED recorders copy a small number of internal signals in a design (to track T_C and Symbolic QED operands) so that we can specify the QED constraints to the BMC tool. For ease of understanding, we take an in-order core with single instruction fetch and 5-stage pipeline as a running example in Section III.C, but we explain how the technique is generalized to other cores. In Section IV, we present results for both in-order (scalar) and OoO (superscalar) cores.

Recorder for T_C. As T_C depends on the starting state chosen by the BMC tool, it cannot be statically determined before the formal analysis begins. A recorder is used to give this information to the BMC tool dynamically. For an in-order core, T_C can be determined by simply tracking the progress of the first Symbolic QED instruction (the first symbolic instruction the BMC tool creates as part of the bug trace) until it reaches the commit stage (write-back stage) of the pipeline. At this time, all SIF instructions must have committed, as the pipeline is occupied by Symbolic QED instructions.

Specifics of the T_C recorder for a 5-stage, single-fetch, in-order pipeline is given in Fig. 5. Inputs are ready signals for all stages that precede the commit stage (e.g., *fetch_ready* is true when the fetch stage is ready to receive an instruction). The output *SIF_complete* is true when the first Symbolic QED instruction goes through all pipeline stages and reaches the commit stage. The output *mode* keeps track of progress made so far by the Symbolic QED instruction (we later make use of this output in the Symbolic QED operand recorder). This T_C recorder for a 5-stage pipeline can be easily modified to support in-order pipelines with a different number of stages.

For an OoO core, the T_C recorder is even simpler, and utilizes the reorder buffer (ROB). The idea is to mark the entry allocated in the ROB for the first Symbolic QED instruction. After this, *SIF_complete* is assigned true when the ROB head pointer reaches the marked instruction. For cores with no ROB, but OoO commit (e.g., [18]), an additional constraint is required (see Section IV).

```
INPUT: fetch_ready, dispatch_ready, exec_ready, mem_ready
OUTPUT: SIF_complete, mode
// initialization
mode ← S0;    SIF_complete ← false;
// end initialization
if (mode == S0) && (fetch_ready) then
  mode ← S1;  SIF_complete ← false;  //inst passes fetch stage
end if
if (mode == S1) && (dispatch_ready) then
  mode ← S2;  SIF_complete ← false;  //inst passes decode stage
end if
if (mode == S2) && (exec_ready) then
  mode ← S3;  SIF_complete ← false;  //inst passes execute stage
end if
if (mode == S3) && (mem_ready) then
  mode ← S4;  SIF_complete ← true;  //inst passes mem stage
end if
```

Fig. 5. Pseudocode for T_C recorder.

Symbolic QED operand recorder. Like T_C, the Symbolic QED operands also depend on the starting state. The Symbolic QED operand recorder stores information for both register and memory operands. Specifics of the Symbolic QED operand recorder for a 5-stage, single-fetch, in-order pipeline is given in Fig. 6. Inputs are: 1) *_*addr*, which gives register/memory address of the corresponding operand; 2) *_*data*, which gives operand data; 3) *_*valid*, which is true when *_*addr* is valid and *_*data* is valid; 4) *mode*, which gives the state of the T_C recorder (Fig. 5). Output *_*buffer* stores all Symbolic QED operands and their values (buffer depth is determined by the maximum number of instructions in-flight at a given time).

```
INPUT: src1_addr, src1_data, src1_valid, src2_addr, src2_data,
src2_valid, mem_addr, mem_data, mem_valid, mode
OUTPUT: src1_buffer, src2_buffer, mem_buffer
// initialization
src1_buffer ← empty_buffer;  src2_buffer ← empty_buffer;
mem_buffer ← empty_buffer;
// end initialization
if (mode != S0) && (mode != S1) && (src1_valid || src2_valid)
then
  if (src1_valid) then
    src1_buffer.add_entry(src1_addr, src1_data);
  end if
  if (src2_valid) then
    src2_buffer.add_entry(src2_addr, src2_data);
  end if
end if
if ((mode == S3) || (mode == S4)) && (mem_valid) then
  mem_buffer.add_entry(mem_addr, mem_data);
end if
```

Fig. 6. Pseudocode for Symbolic QED operand recorder.

We only store the information for Symbolic QED instruction operands in buffers, i.e., we do not store operand information of any SIF instruction. This is enforced by checking the T_C recorder state, i.e., *mode* (we do not add entries to *_*buffer* until all SIF instructions pass through the dispatch stage). In Fig. 6, we assume that each instruction requires at most two register values and one memory value, but the idea is easily extended to more source operands.

For an OoO core, Fig. 6 is extended to include Symbolic QED operands that are waiting on results of earlier Symbolic QED instructions. For each waiting operand, we also store the instruction tag (ROB entry number) of the instruction it is waiting for. This information is used to specify Constraint C-3 for an OoO core (see Appendix C).

IV. Results

In this section, we demonstrate the effectiveness of our new technique on two open-source RISC-V processor cores: i) Vscale [16], an in-order core targeting embedded applications; and ii) RIDECORE [15], an OoO superscalar core (2-way pipeline, 64 maximum instructions in-flight, 2 ALUs, 1 multiplier, 1 load/store unit) for high performance applications. For BMC, we used the Questa Formal tool (version 10.5c) from Mentor Graphics on an AMD Opteron 6438 with 128 GB of RAM. For each core, we instrumented the new QED module (Section III.A), QED constraints (Section III.B), and QED recorders (Section III.C).

A. Previously Unknown Bugs

We first found three previously unknown logic bugs in the multiplier reservation station (RS-m) of the RIDECORE design (all three confirmed by RIDECORE designers [21], see Table 1). These bugs only activate when back-to-back multiply instructions execute on successive clock cycles. They were detected due to the new QED module of this paper (see Section III.A). This design improves upon [6] by allowing arbitrary interleaving of original and duplicate instruction subsequences in EDDI-V tests (see Section II.A), without requiring a waiting period between them. The QED module of [6] cannot detect these bugs, and S^{2}QED [14] is not applicable to RIDECORE.

Table 1. New bugs in RIDECORE. Symbolic QED runtimes.

Bug Activation	Bug Effect	Runtime (symbolic starting state)	Runtime (power-on reset starting state)
All but one (buggy entry) RS-m entries occupied; MULH[4] instruction assigned to vacant entry.	First source operand of MULH instruction corrupted.	25 min.	63 sec.
Same as above.	Second source operand of MULH instruction corrupted.	61 min.	69 sec.
Same as above, but MULHU[5] instr. assigned to vacant entry.	Result of MULHU instruction corrupted.	64 min.	93 sec.

[1]The formal tool is free to choose any values for symbols (state bits) associated with SIF instructions, including those that do not constitute a valid instruction.
[2]Operands may come from either registers or memory locations. For register (memory) operands, the dispatch stage is the register read (memory read) stage.
[3]This condition is required for OoO cores, where there is a possibility that the Symbolic QED operand may wait on a SIF instruction instead of a Symbolic QED instruction.
[4]MULH is a signed multiply instruction selecting the upper half of the multiplier result.
[5]MULHU is an unsigned multiply, selecting the upper half bits of the multiplier result.
[6]This program comes packaged with RIDECORE by the designers as a part of a testbench. It is used only for "extremal" bug creation – not for verification or bug detection.

We also found two bugs in Vscale (Table 2), by running Symbolic QED with the new QED module, starting at a concrete, power-on reset state in less than 40 seconds (also confirmed by designers). These bugs are due to errors in the Vscale implementation of the RISC-V privileged ISA [22], within specific Control Status Registers (CSRs). Importantly, Vscale does not implement shadows for CSRs. To circumvent this, the EDDI-V transformation (Section II.A) duplicates instructions using a scratchpad memory for each CSR.

Table 2. Confirmed bugs in VSCALE. Runtimes are for Symbolic QED with concrete, power-on reset starting state

Bug Activation	Bug Effect	Runtime
'1' is written to specific bit positions in the machine-interrupt CSR MIP.	MTIMECMP register corrupted; Causes repeated interrupts.	2 sec.
Any value with lower two bits '01' or '10' written to the machine-level CSR MSTATUS.	Design enters unspecified privilege level; MEPC corrupted;	33 sec.

B. "Difficult" Logic Bugs and HT Scenarios

We simulated 120 (117) logic bug types using RIDECORE (Vscale). These are "longer" (up to 256 consecutive activation instructions) versions of "difficult" logic bugs (see Appendix A; Table A.1.a-b) that occurred in various commercial designs [6]. We also simulated 195 (156) difficult HT scenarios (see Appendix A; Table A.2.a-c) which encompasses over 100 papers in research literature (see Section V.C) using RIDECORE (V-scale). Results are in Table 3.

Table 3. "Long" logic bugs and HTs. We report [min, avg., max].

		"Long" Bugs	HTs
Vscale	Total count injected	117	156
	Symbolic QED with symbolic starting state		
	Coverage	100%	100%
	Bug trace length (instructions)	[2, 2, 3]	[2, 2, 3]
	Bug trace length (clock cycles)	[5, 5, 6]	[5, 5, 6]
	BMC runtime (seconds)	[2, 4, 25]	[2, 11, 313]
	Symbolic QED with concrete starting state		
	Coverage	33%	15.3%
RIDECORE	Total count injected	120	195
	Symbolic QED with symbolic starting state		
	Coverage	100%	100%
	Bug trace length (instructions)	[4, 4, 4]	[4, 4, 4]
	Bug trace length (clock cycles)	[8, 8, 8]	[8, 8, 8]
	BMC runtime (minutes)	[7, 13, 18]	[7, 20, 121]
	Symbolic QED with concrete starting state		
	Coverage	5%	8.7%

Observation 1: SQED with symbolic starting states correctly and automatically found all "long" logic bugs, in less than 30 mins, with no false positives. It found bugs that traditional BMC methods fail to detect (including SQED). SQED with concrete starting state detected only 5% of these bugs in RIDECORE and 33% of these bugs in Vscale.

Observation 2: SQED with symbolic starting states correctly and automatically found all injected HTs (including those designed to evade state-of-the-art HT detection techniques; see Section V and Appendix A), in less than 2.5 hours, without requiring design-specific assertions or debug of false positives. SQED with a concrete starting state detected only 9% of these HTs in RIDECORE and 15% of these HTs in Vscale.

C. "Extremal" Bugs

To further demonstrate the robustness of our presented technique, we inject "extremal" bugs (only triggered when the design reaches a very specific set of states) into RIDECORE. We focused on RIDECORE for this experiment since it is OoO, superscalar, and more complex than Vscale. Also, S^{2}QED [14] is not applicable to RIDECORE. Our extremal bug injection methodology is as follows: i) Run Matrix Multiply[6] (1M cycles) on the design in simulation, and stop the simulation at a random clock cycle; ii) Run a uniform random sequence of 100 ALU or Load/Store instructions; iii) Select a uniformly random subset of flip-flops from the set of all flip-flops in the design and record their logic values; and iv) Generate a bug (effect A.1.b.3 of Appendix A), injected into the design. This bug activates when the design reaches a state where all the selected flip-flops (step iii) have a specific set of values recorded (step iii).

We present our results in Table 4. For generating such extremal bugs, we randomly chose 180 time points (step i), ranging from 26,026 to 988,159 clock cycles elapsed from program start. For each time point, we ran a random 100-instruction sequence (step ii), and then randomly selected 10 different subsets of 128 flip-flops (step iii), resulting in 1,800 total extremal bug count. Using the Questa Formal tool (version 10.5c) from Mentor Graphics on 6 (in parallel) AMD Opteron 6438 machines with 128 GB of RAM, we were able to run roughly 60 experiments to completion each day. We stopped at 1,800 experiments, after roughly 1 month of runtime.

Whereas Symbolic QED with concrete starting state detected 0% of these 1,800 "extremal" bugs, Symbolic QED with symbolic starting state was able to detect 1,763 of these 1,800 bugs. For the remaining cases, the BMC tool timed out after 24 hours. A closer inspection reveals that the BMC tool was not able to unroll the design beyond 7 clock cycles (8 clock cycles are needed to observe these bugs). In future work, we plan to investigate ways to improve BMC tools to address such issues (following approaches such as [23, 24]).

Table 4. "Extremal" logic bugs in RIDECORE. We report [min, avg., max].

Total count injected	1,800
Symbolic QED with symbolic starting state	
Coverage	97.9%
Bug trace length (instructions)	[4, 4, 4]
Bug trace length (clock cycles)	[8, 8, 8]
BMC runtime (minutes)	[8, 33, 149]
Symbolic QED with concrete starting state	
Coverage	0%

Observation 4: Our new Symbolic QED with symbolic starting states correctly and automatically found 97.9% of the "extremal" logic bugs and generated a bug trace in less than 2.5 hours. In contrast, Symbolic QED with concrete starting state detected 0% of the "extremal" bugs.

V. Related work

In this section, we compare and contrast existing pre-silicon verification techniques for logic bug detection (Section V.A) and HT detection (Section V.B) with the method of this paper. In Section V.C, we provide a survey of HT attacks implemented in research literature. We show that each attack fits in one of

the categories (Appendix A; Tables A.2.a-b) used in our HT experiments (see Section IV.B)

A. *Existing Pre-silicon Verification Methods for Logic Bugs*

Existing formal verification techniques employing BMC [6, 10] have issues in detecting logic bugs that require a long activation sequence. Other works for processor cores use theorem proving [25], or try to learn invariants of the design [26] to be used as constraints, but these techniques tend to be ad-hoc and require a high level of manual effort. In seminal work [27] and extensions [28], models of processors were verified based on abstractions by uninterpreted functions with equality. That approach in general requires to provide invariants to avoid false positives. E-QED [29] is a BMC-based technique for electrical bug localization in *post-silicon* validation. Apart from that, it is substantially different from our technique, e.g., as it does not rely on the duplication of instructions.

False positives are a major challenge for traditional BMC. However, the same QED constraints (Section III.B) used by our approach may not prevent false positives for general property checking using BMC. The following example illustrates this point. Let a processor core start at a state where the Exception Program Counter (EPC) (i.e., the register storing the return address for an exception) is misaligned (i.e., not aligned with any word in the instruction cache), the current PC is within an exception handling routine, and there are only NOP instructions in the pipeline. This is an unreachable state for processors with strict alignment rules (e.g., MIPS [19]). It is reasonable to check the property that the EPC is aligned, since returning to a misaligned address can cause programs to crash. Even at time T_C, when the NOP sequence is finished, this EPC will still be misaligned, causing a false positive. With QED constraints (Section III.B), we do not get such a false positive because the exception handling routine will be filled by valid QED tests. Hence, any time we assert a QED check, it will not fail unless there is a bug in the design.

B. *Existing Pre-silicon Verification methods for HTs*

Existing HT detection techniques that can be applied in pre-silicon verification broadly belong to two categories: i) design analysis methods; and ii) formal methods [30]. One class of design analysis techniques use the observation that signals associated with HTs may be mostly unused or rare. [5, 31-33] use simulation data along with rareness metrics (e.g., code coverage, signal correlation). [34, 35] do not need simulation data, but still trade off false-positives (i.e., spurious detection of HTs) for false-negatives (i.e., failure to detect HTs) and vice-versa, depending on the thresholds set for their rareness metrics.

Table 5. HT Attack(s) implemented in other works

Reference	Trigger(s) from Table A.2.a	IP Block(s) Infected
[50]	a.3	FHT, PID Controller, FPU, PRNG, R-S Decoder
[51]	a.1 (N=3, M_1=32)	AES-128
[52]	a.3 (M_2=4); a.3 (M_2=128)	4-bit ALU, AES-128
[53]	a.1 (N=12, M_1=11); a.1 (N=14, M_1=42)	8051 Microcontroller, UART interface
[54]	a.1 (N=3, M_1=4)	ISCAS'89 benchmarks
[38]	a.4 (X_2=10)	ISCAS'89 benchmarks
[55]	a.3 (M_2=4)	ISCAS'89 benchmarks
[56]	a.3 (M_2=64)	RS232
[57]	a.3 (M_2=16-128)	AES-128
[58]	a.3 (M_2=1)	RSA
[59]	(No Trojans inserted)	DES core
[60]	a.3 (M_2=16); a.3 (M_2=128); a.4 (X_2=128)	DES; AES
[61]	a.2 (X_1=32); a.3 (M_2=8); a.1 (N=4, M_1=8)	RS232
[31]	a.3 (M_2=16); a.3 (M_2=9); a.4 (X_2=7)	ISCAS benchmarks, AES, RS232
[62]	a.3 (M_2=2); a.3 (M_2=4)	ISCAS-85 and ISCAS-89 benchmarks
[63]	a.1 (N=4, M_1=2); a.1 (N=4, M_1=2)	ISCAS-85 and ISCAS-89 benchmarks
[64]	a.1–a.4 (TrustHub and DeTrust)	RS232, AES, Wishbone, BasicRSA
[48]	a.2 (No explicit designs)	AES-128
[65]	a.3 (M_2=36); a.1 (N=2, M_1=2); a.3 (M_2=6)	RS232, ISCAS benchmarks, VGA_LCD
[66]	a.3 (M_2=6)	Elliptic Curve Crypto Core
[43]	a.3 (M_2=4)	8-bit Adder, UART
[67]	a.1 (N=2,4,8, M_1=2,4,8)	AXI4, APB
[68]	a.3 (No explicit designs)	AES-128
[40]	(No explicit designs)	8051 Microcontroller, RC5
[69]	a.1–a.4 (all TrustHub HTs)	All TrustHub benchmarks
[70]	a.1–a.4 (characterizes TrustHub)	All TrustHub benchmarks
[71]	a.1–a.4 (TrustHub, DeTrust), a.2 (XOR- LFSR)	All TrustHub, DeTrust, XOR-LFSR (special case of 1.2)
[32]	(No explicit designs)	Leon3
[72]	a.3 (M_2=1)	Sense-Amplifier
[44]	a.1-a.3 (11 TrustHub Trojans)	AES, RSA
[73]	a.3 (M_2=32)	16-bit Multiplier, 32-bit RSA (both within ARM SoC)
[74]	a.3 (12 HTs of various size)	ISCAS-85 benchmarks
[75]	a.3 (8 HTs of various size)	Alpha encryption module on Spartan-3 FPGA
[45]	a.1-a.4 (Details not sufficient -TrustHUB)	DES encryption core

[41]	a.1-a.4 (Details not sufficient -TrustHub)	8051 Microcontroller
[76]	a.1-a.4 (Details not sufficient -TrustHub)	DES encryption core
[77]	a.1-a.3 (7 HTs)	ISCAS-85 benchmarks
[78]	a.3 (M_2=67,72,152,200)	Two OpenSPARC SRAM modules, Two custom SRAMs
[2]	a.1-a.3	Leon3
[79]	a.1 (N=1, M_1 not given)	UART module
[80]	a.3 (M_2=16)	Virtex-7 FPGA LUT
[81]	a.3 (M_2=2) – generated by two LFSRs	DSP core on Virtex-7 FPGA
[82]	a.2, a.4	64-core SoC on Virtex-7 FPGA
[83]	a.1 (N=1,128,1024,8192, M_1=4,8,32,64,128)	AES-128
[84]	a.2 (X_1=8);	8-LED Marquee Circuit on Spartan-3 FPGA
[85]	a.1 (N=5, M_1=32)	LEON2 Processor
[42]	No HT implemented	Register File Copy Circuit
[86]	a.1-a.4 discussed, but not constructed	32-bit DLX processor
[87]	a.1 (N=30, M_1=1)	Chameleon Cryptography Core
[88]	a.1 (N=4, 16, 64, $M_1 \leq 128$)	ISCAS-89 benchmarks, AES, DCT
[12]	a.1 (N=4, M_1=16); a.1 (N=100, M_1=4); a.3 (M_2=4); a.3 (M_2=128); a.1 (N=4, M_1=128)	8051 Microcontroller, OpenRISC 1200, AES-128
[46]	a.1 (N=4, M_1=128); a.2 (X_1=128); a.3 (M_2=128)	AES, RSA
[89]	a.3 (M_2=16)	Memory controller for 16-bit addressable memory
[90]	a.1 (N=16, M_1=128), TrustHub	Binary Sequence Detector, ISCAS-89, RS232
[13]	a.1-a.4 (TrustHub HTs)	RS232, Wishbone Interconnect, PIC 8-bit, ISCAS-89
[37]	a.3 (M_2=16)	Ethernet MAC 10G circuit
[91]	a.1-a.4 (19 TrustHub HTs)	TrustHub benchmarks
[49]	a.3	ISCAS-85 benchmarks
[92]	a.1 (No explicit construction)	Attack on processor data memory
[93]	a.3 (No details given)	MPEG and 5 DSP accelerators (C programs)
[94]	a.3 (M_2=1)	11 Different Arithmetic, DSP cores (C-code accelerators)
[95]	a.3 (M_2=1)	IIR Filter Accelerator (C program)
[96]	a.3 (M_2=64); (4 HTs)	Ethernet MAC 10G circuit
[97]	a.1-a.4 (details not given; 7 HTs)	TEA encryption on FPGA
[39]	a.1-a.4 (details not given; 37 HTs)	ITC-99 benchmarks (slightly modified)
[98]	(No explicit designs given)	ISCAS-85 and ISCAS-89 benchmarks
[99]	a.3 (M_2 arbitrary)	Leon3
[100]	a.1–a.4 (9 HTs)	RS232 serial interface
[101]	a.3 (M_2=64); a.3 (M_2=32)	DES, XTEA, CA PRNG
[102]	a.1; a.3(M_2=32); a.3(M_2=10)	Sobel filter, AES, UART (C-code accelerators)
[103]	a.1; a.2	OpenSPARC T2
[104]	a.1; a.2; a.3	OpenSPARC T2
[34]	a.1-a.4 (TrustHub benchmarks)	TrustHub benchmark circuits
[105]	a.1; a.2 (no explicit designs given)	4-bit adder circuit
[106]	a.1 (N=3, M_1=16); 10 HTs	8051 Microcontroller
[107]	a.3 (single extra inverter, 8 HTs)	ISCAS-89 benchmarks, SoC (32-bit DLX core, AES, FFT)
[108]	a.3 (single extra gate, 10 HTs)	ISCAS-85, ISCAS-89 and ITC-99 benchmarks
[109]	a.3 (single extra gate, 10 HTs)	ISCAS-85, ISCAS-89, and ITC-99 benchmarks
[110]	a.3 (single extra gate, 10 HTs)	ISCAS-85, ISCAS-89, and ITC-99 benchmarks
[35]	a.1–a.3	OpenRISC 1200, Wishbone, Basic RSA, AES, ISCAS'89
[5]	a.1–a.4	RS232
[36]	a.1–a.4	8051 Microcontroller, OpenRISC 1200, RS232
[11]	a.1 (N=3, M_1=4)	OpenRISC 1200, Wishbone interconnect, ISCAS'89
[111]	a.1–a.4 (20 TrustHub benchmarks)	OpenRISC 1200, LEON3, RS232, ISCAS benchmarks
[112]	a.3 (M_2=128)	AES-128

Additionally, stealthy HTs have been designed [11] to bypass such analyses. In contrast to that, our technique does not require simulation data, detects stealthy HTs given in [11, 36-37], and does not produce any false positives. However, our technique is for processor cores, while the aforementioned analysis techniques are applicable for general designs.

Formal methods for finding HTs generally either use BMC [12, 16], SAT-based equivalence checking [13, 38-39] or theorem proving [40-42]. These techniques face similar challenges to BMC-based techniques for logic bug detection, in addition to manual creation of properties.

Complementary approaches to ours include techniques to detect HTs that leak sensitive data, but do not produce incorrect logic values [43-46], and HT prevention methods [47-49].

C. Literature Survey of Implemented HT Attacks

To confirm that our list of HTs (Appendix A; Table A.2.a-b) is representative, we surveyed over 100 different papers which categorize and/or construct example HTs for experimental evaluation. All explicit HT constructions are shown in Table 5 (with parameters given, if noted explicitly in the paper). Many of the papers use a large subset of the TrustHub [37] or DeTrust [11] benchmarks. Both of these benchmarks are covered by HT activation criteria from Table A.2.a. Additional papers [113-132] not included in Table 5 are surveys or papers that describe attacks in words. We confirmed that there are no HT attack types in [113-132] that we do not encompass.

VI. Conclusion

In this paper, we extended Symbolic QED to include symbolic starting states. As a result, we overcome limitations of existing pre-silicon verification techniques for detecting logic bugs and HTs that require long activation sequences. The unique combination of Symbolic QED and QED constraints enable us to achieve this objective. Our results on multiple open-source RISC-V processor cores demonstrate the effectiveness and practicality of our approach: i) detection of previously unknown logic bugs within minutes; ii) detection of 100% of hundreds of long logic bugs and HTs (SQED with a concrete starting state detects, at best, 33%); iii) detection of 97.9% of "extremal" logic bugs (SQED with a concrete starting state detects 0%). Future research directions include: i) extending our approach to detect bugs and HTs in other SoC components beyond processor cores, such as uncore components and accelerators; ii) handling other QED transformations beyond EDDI-V, e.g., CFTSS-V and CFCSS-V [6]; iii) automated methods for inserting QED recorders and generating QED constraints on the symbolic starting state; iv) theoretical comparison of the bug detection capabilities of [6], [14], and the method of this paper.

Appendix A: Logic Bug and Hardware Trojan Types

In the following tables, we give the different logic bug (harder versions of "difficult" bugs that occurred in various commercial designs [6]) and HT scenarios (from research literature) used in Table 3 of Section IV. Each "long" logic bug is modeled with two parts: i) activation criteria of the bug (Table A.1.a), i.e., the conditions which need to be satisfied for the bug to activate; and ii) effect of the bug once it is activated (Table A.1.b). For our experiments, we considered a whole range of values for the parameters in Table A.1, as follows, N=Y={2, 4, 8, 16, 32, 64, 128, 256}, R=X={2, 4, 6, … , 30}. This results in a total of 117 logic bugs in Vscale (A.1.a.5 is not possible), and 120 logic bugs in RIDECORE.

Table A.2.a gives HT activation types used in Table 3 of Section IV. Table A.2.b gives various effects an HT can have on the executing instructions [2]. Table A.2.c presents three HT implementation techniques used to inject HTs in designs [12]. We create stealthy HTs that are known to evade common detection techniques (e.g., HT designs from [36] evade detection techniques based on UCI [32] and coverage metrics [5, 32]). A HT scenario is formed by using one activation criteria (Table A.2.a) with one bug effect (Table A.2.b), along with an appropriate design strategy (Table A.2.c). We used a wide range of HT scenario parameters, given in Table A.2: N={2, 4, 8, … , 256}, M_1=32, X_1=X_2={128, 256}, M_2=64, resulting in 156 HT scenarios in Vscale (effect A.2.b.5 is not possible) and 195 HT scenarios in RIDECORE. These values make HTs harder to activate than benchmark HTs in [37].

Logic bugs and HTs were injected by introducing a small state machine into the design that checks for the activation criteria, and flips bits at desired wires to achieve the effect.

Table A.1.a. Activation criteria for "long" logic bugs.

Processor Core	1. Data forwarding between pipeline stages.
	2. Two specific instructions within X cycles.
	3. R registers must all contain value V.
	4. A specific sequence of N instructions must execute within Y cycles.
	5. A specific cache state.

Table A.1.b. Bug effect from [6].

Processor Core	1. Next instruction corrupted to NOP.
	2. Next instruction opcode incorrectly decoded.
	3. Next instruction register read corrupted.

Table A.2.a. Activation criteria for HTs from [37].

Processor Core	1. Specific length N sequence on M_1 internal wires.
	2. X_1 bit counter reaching final value.
	3. Comparator on M_2 internal wires becomes true.
	4. X_2 bit rare event counter reaches a specific value.

Table A.2.b. HT effects.

Processor Core	1. An in-flight instruction changed to NOP.
	2. Opcode of an in-flight instruction changed.
	3. Next register read corrupted.
	4. Next result of an execution unit changed.
	5.Corrupts ROB. Prematurely commits next inst.

Table A.2.c. HT design techniques.

Method	HT stealthy against following techniques
[37]	Traditional pre-silicon verification.
[36]	UCI [32]; coverage metrics [5, 32].
[11]	[5, 32, 33, 34].

Appendix B: Mathematical Proofs

In this Appendix, we formalize our assumptions on how any bug-free design should operate. We relate these assumptions to Section III.B, and prove Theorem 1.

We first provide preliminary definitions [133]. We will use the term *alphabet* to refer to a nonempty set of symbols. We will often be dealing with operations on *words* (sequences of symbols from countable alphabets). We will denote the empty word as ε, and if w and v are two words over the same alphabet, we denote their concatenation as wv. For finite vectors of equal length, $\mathbf{x} = (x_1, \ldots, x_N)$ and $\mathbf{y} = (y_1, \ldots, y_N)$, we write $\Delta(\mathbf{x}, \mathbf{y})$ for the subset of indices they differ on.

The next definition provides the most general model of the computation used in our statements.

Definition 1 (Transition System)**.** A tuple $\mathbb{T} = \langle \mathcal{S}, \mathcal{S}_0, \mathbb{I}, \mathcal{T}, \mathcal{F} \rangle$ is called a *transition system* if

- $\mathcal{S}$ is a countable alphabet of *states*.

- $\mathcal{S}_0 \subseteq \mathcal{S}$ is the nonempty subset of *initial* states.
- $\mathbb{I}$ is a nonempty, finite set of actions.
- $\mathcal{T} \subseteq \mathcal{S} \times \mathbb{I} \times \mathcal{S}$ is the *transition relation*.
- $\mathcal{F} \subseteq \mathcal{S}$ is the nonempty subset of *accept* states.

For each transition system, we also associate a specification function $Spec$: $\mathcal{S} \times \mathbb{I} \to \mathcal{S}$. This is the function such that

$$s_1 = Spec(s_0, I) \Leftrightarrow \langle s_0, I, s_1 \rangle \in \mathcal{T}.$$

The *state-space* $\mathcal{S}$ contains all states that can be represented by the transition system. $\mathcal{S}_0$ is the set of states that the transition system can begin in for any execution. $\mathbb{I}$ is a set of actions that can be applied to steer the system from one state to the next. $\mathcal{T}$ is the transition relation, a countable set which represents the mapping that each action implements. $\mathcal{F}$ is a set of accept states, in which executions can end.

The next definition describes finite sequences of actions, and the states they allow a system to traverse.

Definition 2 (Path)**.** A *path* or *trace* of length K in a transition system $\mathbb{T} = \langle \mathcal{S}, \mathcal{S}_0, \mathbb{I}, \mathcal{T}, \mathcal{F} \rangle$ is a pair $\left(s_0, \{I_i\}_{i=1}^{K}\right)$, where

i. $s_0 \in \mathcal{S}_0$ is an initial state.
ii. $\{I_i\}_{i=1}^{K}$ is an action sequence, where $I_i \in \mathbb{I}$, for $1 \le i \le K$.
iii. $\langle s_i, I_{i+1}, s_{i+1} \rangle \in \mathcal{T}$, for $0 \le i \le K-1$.

A path may also be denoted explicitly by the sequence of states traversed as

$$s_0 \xrightarrow{I_1} s_1 \xrightarrow{I_2} \cdots \xrightarrow{I_{K-1}} s_{K-1} \xrightarrow{I_K} s_K.$$

For any processor core, we assume there exists a transition system model (with finite state-space) that defines the behavior of the system. We call this transition system the *ISA* (e.g., [134, 135]) of the core. The actions in an ISA are called *instructions*. This concept is formalized in the next definition.

Definition 3 (ISA)**.** A transition system $\mathbb{T} = \langle \mathcal{S}, \mathcal{S}_0, \mathbb{I}, \mathcal{T}, \mathcal{F} \rangle$ with finite state-space $\mathcal{S}$ is called an *ISA* with $N \ge 1$ *original* registers and $Q \ge 1$ *original* memory locations if

i. $\mathcal{S} = \left(R_1, \ldots, R_{2N}, M_1, \ldots, M_{2Q}, \mathbf{Z}\right)$ is the state space.
ii. $\left(R_1, \ldots, R_{2N}, M_1, \ldots, M_{2Q}\right)$ is called *architectural* state.
iii. $\mathbf{Z}$ is the *internal* state.
iv. $R_1, \ldots, R_N$ are *original registers*. $R_{N+1}, \ldots, R_{2N}$ are *duplicate registers*. Registers can take any value from a finite alphabet, $\mathcal{R}$.
v. $M_1, \ldots, M_Q$ are *original memory* and $M_{Q+1}, \ldots, M_{2Q}$ are *duplicate memory*. Memories can take any value from a finite alphabet, $\mathcal{M}$.
vi. Each instruction $I \in \mathbb{I}$, has a set of *source operands*, and a set of *destination operands*.
vii. R_k is a source operand of $I \in \mathbb{I}$ iff. $\exists\, s_0, s_1 \in \mathcal{S}$, with corresponding architectural states a_0, a_1 st.,
$Spec(s_0, I) \neq Spec(s_1, I)$, and $\Delta(a_0, a_1) = k$.
Likewise, M_j is a source operand of $I \in \mathbb{I}$ iff. $\exists\, s_0, s_1 \in \mathcal{S}$, with corresponding architectural states a_0, a_1 st.,
$Spec(s_0, I) \neq Spec(s_1, I)$, and $\Delta(a_0, a_1) = 2N + j$.
viii. A register or memory location is a destination operand for $I \in \mathbb{I}$ if there exists $\langle s_0, I, s_1 \rangle \in \mathcal{T}$ such that s_0 and s_1 differ on these indices**.**

Instructions having only original registers and memory as *both* source and destination operands are called *original instructions*. Likewise, instructions using only duplicate registers and memory as operands are called *duplicate instructions*. An instruction is considered a *NOP* if both source and destination operands are $\emptyset$.

Note, there is no loss of generality in this hard-coding of the architectural state indices. We can always define two permutations, σ and μ on $[1, \ldots, 2N]$ and $[1, \ldots, 2Q]$ respectively, s.t. $\mathcal{S} = \left(R_{\sigma(1)}, \ldots, R_{\sigma(2N)}, M_{\mu(1)}, \ldots, M_{\mu(2Q)}, \mathbf{Z}\right)$.

Definition 3 is general enough to handle instructions with multiple destination operands. So, superscalar cores which commit multiple instructions per cycle are still covered.

Now we prove Theorem 1 of Section III.B.

Proof of Theorem 1: Let $\left(s_0, \{J_i\}_{i=1}^{K}\right)$ be a bug trace obtained from SQED with symbolic starting states, denoted as:

$$s_0 \xrightarrow{J_1} s_1 \xrightarrow{J_2} \cdots \xrightarrow{J_{Tc}} s_{Tc} \xrightarrow{O_1} \cdots \xrightarrow{D_n} s_K.$$

Here, $\{J_i\}_{i=1}^{Tc}$ are the symbolic in-flight instructions and s_{Tc} is a QED-consistent state (see Constraint C-2). Without loss of generality, assume the original, duplicate register and memory pairs for EDDI-V are chosen as (R_i, R_{i+N}), for $1 \le i \le N$ and (M_j, M_{j+Q}), for $1 \le j \le Q$.

Let $\{O_i\}_{i=1}^{n}$ be the subsequence of original instructions and $\{D_i\}_{i=1}^{n}$ be the subsequence of duplicate instructions in the failing EDDI-V test. Indexing in the subsequences corresponds to the order in which instructions commit to architectural state.

Without loss of generality, assume the failed EDDI-V test is due to mismatched values in two registers (R_i, R_{i+N}), as opposed to memory. Let $val(s, R_i)$ denote the value held by register R_i in state s. Because s_{Tc} is QED-consistent,

$$val(s_{Tc}, R_i) = val(s_{Tc}, R_{i+N}).$$

Further, it must be true that

$$\exists a \in \{1, \ldots, n\} \text{ st. } \left(val(s_{T_{Oa}}, R_i) \neq val(s_{T_{Da}}, R_{i+N})\right) \wedge \left(\wedge_{b \in \{1,\ldots,a-1\}} val(s_{T_{Ob}}, R_i) = val(s_{T_{Db}}, R_{i+N})\right), \quad (1)$$

where T_{Oa} is the time where O_a writes (commits) to destination operand R_i and T_{Da} is the time where D_a writes to destination operand R_{i+N}. Explicitly, (O_a, D_a) is the first pair of SQED instructions that force these two architectural state elements to be QED inconsistent. Equation (1) is true because there must exist some Symbolic QED instructions which write to the pair R_i, R_{i+N} such that the QED check fails on s_K, as Constraint C-1 ensures that all SIF instructions complete by T_C.

We can partially represent instructions O_a and D_a as below:

$$O_a : R_i \leftarrow \text{op } x_1, x_2, \ldots, x_m$$
$$D_a : R_{i+N} \leftarrow \text{op } x'_1, x'_2, \ldots, x'_m.$$

Here, op is a function performed on data stored in source operands $x_1, \ldots, x_m$, and each instruction writes a computed result to its destination operand. Because O_a, D_a are a pair of Symbolic QED instructions, they implement the same function on the source operands.

When O_a and D_a execute, *only one* of two conditions are satisfied:

(A) $\forall j \in \{1, \ldots, m\}, \quad val(s_{T_{Oa}-1}, x_j) = val(s_{T_{Da}-1}, x'_j)$.
(B) $\exists j \in \{1, \ldots, m\}$ st. $val(s_{T_{Oa}-1}, x_j) \neq val(s_{T_{Da}-1}, x'_j)$.

First, assume **(A)** holds. Then all source operand data of O_a and D_a match:

$$O_a : R_i \leftarrow \text{op } data_1, data_2, \ldots, data_m$$
$$D_a : R_{i+N} \leftarrow \text{op } data_1, data_2, \ldots, data_m.$$

However, we also know that $val(s_{T_{Da}}, R_i) \neq val(s_{T_{Da}}, R_{i+N})$ because an EDDI-V test failed. This implies that the same operation (op) performed on the same data results in two different values when executed twice, contradicting *Assumption-1* of any bug-free design. Therefore, for case **(A)**, Theorem 1 holds.

Next, assume **(B)** holds instead of **(A)**. Depending on when the operands' data are available for the instructions to compute on, we have five mutually disjoint subcases for **(B)** (for each subcase, we show that Theorem 1 holds):

(B.1) At T_C, data for both operands x_j and x'_j is available.

As Constraint C-3 (i) holds, we know that $val(s_{T_C}, x_j) = val(s_{T_{Oa}-1}, x_j)$, and $val(s_{T_C}, x'_j) = val(s_{T_{Da}-1}, x'_j)$. From Constraint C-2, s_{T_C} is also QED-consistent. Therefore, by transitivity of equality, $val(s_{T_{Oa}-1}, x_j) = val(s_{T_{Da}-1}, x'_j)$. This contradicts the assumption of **(B)**. Thus, case **(B.1)** cannot arise when QED constraints are in place.

(B.2) At T_C, data for only one operand (pick x_j without loss of generality) is available.

If **(B.2)** holds, *only one* of the following two cases can arise: **(B.2.1)** There are no earlier (before D_a) SQED instructions writing to x'_j; or **(B.2.2)** There is at least one earlier SQED instruction upon which D_a has RAW dependency for source operand x'_j.

Assume case **(B.2.1)** holds. From Constraints C-3 (i) and C-2, $val(s_{T_C}, x_j) = val(s_{T_{Oa}-1}, x_j)$ and $val(s_{T_C}, x_j) = val(s_{T_C}, x'_j)$. If *Assumption-2* holds, we have $val(s_{T_{Da}-1}, x'_j) = val(s_{T_C}, x'_j)$, which implies by transitivity of equality that $val(s_{T_{Oa}-1}, x_j) = val(s_{T_{Da}-1}, x'_j)$. However, this contradicts the assumption of **(B)**. Thus, for case **(B.2.1)**, if a QED test fails, it is caused by a bug in the design.

Now assume that **(B.2.2)** holds instead of **(B.2.1)**. Let D_y be the last instruction that D_a has RAW dependency on for source operand x'_j. From *Assumption-2*, we have $val(s_{T_{Dy}}, x'_j) = val(s_{T_{Da}-1}, x'_j)$. Let O_y be the corresponding original instruction for D_y. Note that O_a also has an equivalent RAW dependency upon O_y. Therefore, from *Assumption-2* we again have $val(s_{T_{Oy}}, x_j) = val(s_{T_{Oa}-1}, x_j)$. We also have from equation (1), $val(s_{T_{Oy}}, x_j) = val(s_{T_{Dy}}, x'_j)$. Hence, by transitivity of equality, $val(s_{T_{Oa}-1}, x_j) = val(s_{T_{Da}-1}, x'_j)$. However, this contradicts the assumption of **(B)**, Thus, for case **(B.2.2)**, if a QED test fails, it is caused by a bug in the design.

(B.3) At T_C, data for both operands x_j and x'_j are not available.

If case **(B.3)** holds, *only one* of two cases can arise: **(B.3.1)** There is no earlier (before O_a, D_a) SQED instruction pair that write to x_j, x'_j; **(B.3.2)** There is an earlier SQED instruction pair O_y, D_y that write to x_j, x'_j that is the last pair O_a, D_a have RAW dependencies on for these operands.

Next, assume that **(B.3.1)** holds. From *Assumption-2*, we have $val(s_{T_C}, x_j) = val(s_{T_{Oa}-1}, x_j)$ and $val(s_{T_C}, x'_j) = val(s_{T_{Da}-1}, x'_j)$. From Constraint C-2, we also know that $val(s_{T_C}, x_j) = val(s_{T_C}, x'_j)$. Thus, by transitivity of equality, we have $val(s_{T_{Oa}-1}, x_j) = val(s_{T_{Da}-1}, x'_j)$, but this contradicts **(B)**. Hence, in case **(B.3.1)** we also conclude that if a QED property fails, it is caused by a bug in the design.

Finally, assume that **(B.3.2)** holds. From *Assumption-2* we know that $val(s_{T_{Oy}}, x_j) = val(s_{T_{Oa}-1}, x_j)$ and $val(s_{T_{Dy}}, x'_j) = val(s_{T_{Da}-1}, x'_j)$. From Eqn. (1), $val(s_{T_{Oy}}, x_j) = val(s_{T_{Dy}}, x'_j)$, and then by transitivity, we have $val(s_{T_{Oa}-1}, x_j) = val(s_{T_{Da}-1}, x'_j)$. This contradicts **(B)**. Thus, for **(B.3.2)** we also conclude that if a QED test fails, it is caused by a bug in the design.

We have shown that in each of the six possible mutually disjoint cases, a QED test failure can only be caused by a bug in the design. This proves Theorem 1. ■

APPENDIX C: SPECIFYING QED CONSTRAINTS DURING BMC

In this Appendix, we describe in detail how we specify the QED constraints (see Section III.B) to the BMC tool.

Specifying C-1. Constraint C-1 is naturally satisfied in processors with in-order execution, which is the case for processors with in-order pipelines. But, this is not the case with OoO cores. This is due to instruction indirection, i.e., renaming of instructions using respective ROB entries to support OoO execution. When starting at a symbolic state, ROB entry locations for SIF instructions may be chosen by the BMC tool such that SIF instructions commit after QED instructions, thereby violating C-1. So, specifying C-1 just requires constraining ROB entries for SIF instructions to avoid the issue.

Specifying C-2. Constraint C-2 requires that test modes such as scan which can bypass instructions and write directly to the architectural state need to be turned off at T_C (otherwise, spurious counterexamples can occur). Assuming there is a $\mathrm{Test}_{\mathrm{enable}}$ signal to turn on/off each scan or other test mode, we can specify C-2 using the T_C recorder (Fig. 5) and the below statements:

$$\uparrow(\mathrm{SIF}_{\mathrm{complete}}) \Rightarrow \forall(i,j) \in \Lambda_R, (R_i == R_j),$$
$$\uparrow(\mathrm{SIF}_{\mathrm{complete}}) \Rightarrow \forall(m,n) \in \Lambda_M, (M_m == M_n),$$
$$\uparrow(\mathrm{Clock}) \Rightarrow \mathrm{if}\,(\mathrm{SIF}_{\mathrm{complete}}), \mathrm{Test}_{\mathrm{enable}} == 0.$$

Above, $\uparrow(\mathrm{Signal}_{\mathrm{name}})$ is true on any clock edge where $\mathrm{Signal}_{\mathrm{name}}$ transitions from low to high; Λ_R is the set of all mapped (original, duplicate) pairs of registers; R_i is the value held in register i; Λ_M is the set of all mapped (original, duplicate) pairs of memory locations; and M_m is the value held in memory location m. For the experiments in Section IV, these statements were specified in the form of System-Verilog *assume statements*. Note that these constraints take the same form for both in-order and OoO cores.

Specifying C-3. Constraint C-3(ii) is vacuously true for in-order pipelines, as an instruction only makes progress when all its operands have already read their respective data. Otherwise, the instruction just stalls for operand data. We use the T_C (Fig. 5) and SQED operand (Fig. 6) recorders to specify C-3(i):

$$\uparrow(\mathrm{SIF}_{\mathrm{complete}}) \Rightarrow \forall s \in \mathrm{src1\_buffer}\ (s.\mathrm{data} == R_{s.\mathrm{addr}}),$$
$$\uparrow(\mathrm{SIF}_{\mathrm{complete}}) \Rightarrow \forall s \in \mathrm{src2\_buffer}\ (s.\mathrm{data} == R_{s.\mathrm{addr}}),$$
$$\uparrow(\mathrm{SIF}_{\mathrm{complete}}) \Rightarrow \forall m \in \mathrm{mem\_buffer}\ (m.\mathrm{data} == M_{m.\mathrm{addr}}).$$

Above, s.data gives the data stored for entry s in the buffer and s.addr gives the address. R_i is the value held in register i; and M_m is the value held in memory location m. For an OoO core, specifying C-3(i) is the same as above, but also checks additional ROB data in the Symbolic QED operand recorder (see Section III.C).

Finding Counterexamples Using BMC. The property (see Section II.B) used by BMC to find counter-examples in Symbolic QED is modified, using the T_C recorder (Fig. 5) to support symbolic starting states:

$$\uparrow(\mathrm{QED}_{\mathrm{ready}}\ \&\&\ \mathrm{SIF}_{\mathrm{complete}}) \Rightarrow \bigwedge_{a \in \{1,\ldots,\frac{N}{2}\}} \mathrm{Ra} == \mathrm{Ra}'$$

Here, the only change is the addition of the $\mathrm{SIF}_{\mathrm{complete}}$ pre-condition to the QED property.

REFERENCES

[1] H. D. Foster, "Trends in functional verification: A 2014 industry study," Proc. *DAC*, 2015.

[2] S. T. King et al., "Designing and implementing malicious hardware," *LEET*, 2008.

[3] R. Karri et al., "Trustworthy hardware: identifying and classifying hardware Trojans," *Computer*, 42(10):39-46, 2010.

[4] T. F. Wu et al., "TPAD: hardware Trojan prevention and detection for trusted integrated circuits," *IEEE Trans. CAD*, 35(4):521-534, 2016.

[5] X. Zhang and M. Tehranipoor, "Case study: detecting hardware Trojans in third-party digital IP cores," Proc. *HOST*, 2011.

[6] E. Singh et al., "Logic bug detection and localization using symbolic quick error detection," *IEEE Trans. CAD*, 2018.

[7] D. Lin et al., "Effective post-silicon validation of system-on-chips using quick error detection," *IEEE Trans. CAD*, 33(10):1573-1590, 2014.

[8] E. Clarke et al., "Bounded model checking using satisfiability solving," *Formal Methods in System Design*, 19(1):7-34, 2001.

[9] E. Singh et al., "Symbolic QED pre-silicon verification for automotive microcontroller cores: industrial case study," Proc. *DATE*, 2019.

[10] A. Reid et al., "End-to-end verification of processors with ISA-Formal," Proc. *CAV*, 2016.

[11] J. Zhang et al., "Detrust," Proc. *CCCS*, 2014.

[12] J. V. Rajendran, V. Vedula, and R. Karri, "Detecting malicious modifications of data in third-party intellectual property cores," Proc. *DAC*, 2015.

[13] T. Reece and W. H. Robinson, "Detection of hardware Trojans in third-party intellectual property using untrusted modules," *IEEE Trans. CAD*, 35(3):357-366, 2016.

[14] M. R. Fadiheh et al., "Symbolic quick error detection using symbolic initial state for pre-silicon verification," Proc. *DATE*, 2018.

[15] "RIDECORE," https://github.com/ridecore/ridecore.

[16] "V-scale," https://github.com/ucb-bar/vscale.

[17] A. Biere et al., "Symbolic model checking without BDDs," Proc. *TACAS*, 1999.

[18] "Aquarius," opencores.org/projects/aquarius.

[19] K. Yeager, "The MIPS R10000 superscalar microprocessor," *IEEE Micro*, 16(2):28-41, 1996.

[20] "Cortex-A15," https://tinyurl.com/y75sejwz.

[21] "Issue: bugs in rs_mul," https://tinyurl.com/y8otzyxb.

[22] "Privileged Architecture," https://tinyurl.com/y8jgqqza.

[23] M. K. Ganai, A. Gupta, and P. Ashar, "Efficient modeling of embedded memories in bounded model checking," Proc. *CAV*, 2004.

[24] M. K. Ganai and A. Gupta, "Accelerating high-level bounded model checking," Proc. *ICCAD*, 2006.

[25] J. Bhadra et al., "A survey of hybrid techniques for functional verification," *IEEE Design & Test of Computers*, 24(2):112-122, 2007.

[26] M. Thalmaier et al., "Analyzing k-step induction to compute invariants for SAT-based property checking," Proc. *DAC*, 2010.

[27] J. R. Burch and D. Dill, "Automatic verification of pipelined microprocessor control," Proc. *ICCAD*, 1994.

[28] S. Berezin et al., "Combining symbolic model checking with uninterpreted functions for out-of-order processor verification," Proc. *FMCAD*, 1998.

[29] E. Singh et al., "E-QED: electrical bug localization during post-silicon validation enabled by quick error detection and formal methods," Proc. *CAV*, 2017.

[30] K. Xiao et al., "Hardware Trojans: lessons learned after one decade of research," *TODAES*, 22(1), May 2016.

[31] B. Cakir and S. Malik, "Hardware Trojan detection for gate-level ICs using signal correlation-based clustering," Proc. *DATE*, 2015.

[32] M. Hicks et al., "Overcoming an untrusted computing base: detecting and removing malicious hardware automatically," Proc. *SSP*, 2010.

[33] J. Zhang et al., "VeriTrust," Proc. *DAC*, 2013.

[34] A. Waksman et al., "FANCI: Identification of stealthy malicious logic using Boolean functional analysis," Proc. *CCCS*, 2013.

[35] S. Yao et al., "FASTrust," Proc. *ITC*, 2015.

[36] J. Zhang et al., "On hardware Trojan design and implementation at register-transfer level," Proc. *HOST*, 2013.

[37] H. Salmani, M. Tehranipoor, and R. Karri, "On design vulnerability analysis and trust benchmarks development," Proc. *ICCAD*, 2013.

[38] M. Banga and M. S. Hsiao, "Trusted RTL: Trojan detection methodology in pre-silicon designs," Proc. *HOST*, 2010.

[39] G. Shrestha and M. S. Hsiao, "Ensuring trust of third-party hardware design with constrained sequential equivalence checking," Proc. *IEEE Conf. on Tech. for Homeland Security*, 2012.

[40] X. Guo et al., "Eliminating the hardware-software boundary: a proof-carrying approach for trust evaluation on computer systems," *IEEE Trans. Inf. Forensics Security*, 12(2):405-417, 2017.

[41] Y. Jin and Y. Makris, "A proof-carrying based framework for trusted microprocessor IP," Proc. *ICCAD*, 2013.

[42] E. Love, Y. Jin, and Y. Makris, "Proof-carrying hardware intellectual property: A pathway to trusted module acquisition," *IEEE Trans. Inf. Forensics Security*, 7(1):25-40, 2012.

[43] N. Fern, I. San, and K. T. T. Cheng, "Detecting hardware Trojans in unspecified functionality through solving satisfiability problems," Proc. *ASP-DAC*, 2017.

[44] W. Hu et al., "Detecting hardware Trojans with gate-level information-flow tracking," *Computer*, 49(8):44-52, 2016.

[45] Y. Jin and Y. Makris, "Proof carrying-based information flow tracking for data secrecy protection and hardware trust," Proc. *VTS*, 2012.

[46] J. V. Rajendran et al., "Formal Security Verification of Third-Party Intellectual Property Cores for Information Leakage," Proc. *Intl. Conf. on VLSI Design*, 2016.

[47] R. S. Chakraborty and S. Bhunia, "HARPOON: an obfuscation-based SoC design methodology for hardware protection," *IEEE Trans. CAD*, 28:1493-1502, 2009.

[48] S. Dupuis et al., "A novel hardware logic encryption technique for thwarting illegal overproduction and hardware Trojans," Proc. *IOLTS*, 2014.

[49] M. S. Samimi et al., "Hardware enlightening: nowhere to hide your Hardware Trojans!" Proc. *IOLTS*, 2016.

[50] A. Al-Anwar et al., "Hardware Trojan protection for third party IPs," Proc. *Euromicro Conf. on Digital Sys. Design*, 2013.

[51] S. S. Ali et al., "Multi-level attacks: An emerging security concern for cryptographic hardware," Proc. *DATE*, 2011.

[52] H. Amin et al., "System-level protection and hardware Trojan detection using weighted voting," *J. Advanced Research*, 5(4):499-505, 2014.

[53] J. Backer, et al., "Reusing the IEEE 1500 design for test infrastructure for security monitoring of Systems-on-Chip," *DFT*, pp. 52-56, 2014.

[54] M. Banga and M. S. Hsiao, "A novel sustained vector technique for the detection of hardware Trojans," *VLSI Design*, pp. 327–332, 2009.

[55] M. Banga and M. S. Hsiao, "ODETTE: A non-scan design-for-test methodology for Trojan detection in ICs," Proc. *HOST*, 2011.

[56] A. Baumgarten et al., "A case study in hardware Trojan design and implementation," *Intl. J. Info. Security*, 10(1):1-14, 2011.

[57] S. Bhasin et al., "Hardware Trojan horses in cryptographic IP cores," *FDTCS*, 2013.

[58] S. Bhunia et al., "Protection against hardware trojan attacks: Towards a comprehensive solution," *IEEE Design & Test*, 30(3):6-17, 2013.

[59] M.-M. Bidmeshki and Y. Makris, "Toward automatic proof generation for information flow policies in third-party hardware IP," Proc. *HOST*, 2015.

[60] M.-M. Bidmeshki et al., "Data secrecy protection through information flow tracking in proof-carrying hardware IP—part II: framework automation," *IEEE Trans. Info. Forensics and Security*, 12(10):2430-2443, 2017.

[61] C. Bobda et al., "Hardware sandboxing: a novel defense paradigm Against hardware Trojans in systems on chip," Proc. *ARC*, 2017.

[62] R. S. Chakraborty et al., "MERO: A statistical approach for hardware Trojan detection," Proc. *CHES*, 2009.

[63] R. S. Chakraborty et al., "Security against hardware Trojan attacks using key-based design obfuscation," *J. Elect. Test*, 27:767–785, 2011.

[64] X. Chen et al., "Hardware Trojan detection in third-party digital intellectual property cores by multilevel feature analysis," *IEEE Trans. CAD*, 37(7):1370-1383, 2018.

[65] F. Farahmandi, Y. Huang, and P. Mishra, "Trojan localization using symbolic algebra," Proc. *ASP-DAC*, 2017.

[66] N. Fern, S. Kulkarni, and K. T. T. Cheng, "Hardware Trojans hidden in RTL don't cares - automated insertion and prevention methodologies," Proc. *ITC*, 2015.

[67] N. Fern et al., "Hiding hardware Trojan communication channels in partially specified SoC bus functionality," *IEEE Trans. CAD,* 36(9):1435-1444, 2017.

[68] X. Guo et al., "Automatic RTL-to-Formal code converter for IP security formal verification," Proc. *MTV*, 2016.

[69] S. K. Haider et al., "Hatch: A formal framework of hardware trojan design and detection," *Univ. Connecticut, Cryptol. ePrint Arch., Tech. Rep* 943, 2014.

[70] S. K. Haider, C. Jin, and M. Dijk, "Advancing the state-of-the-art in hardware Trojans design," Proc. *MWSCAS*, 2017.

[71] S. K. Haider et al., "Advancing the state-of-the-art in hardware Trojans detection," *IEEE Trans. Dependable and Secure Computing*, 16(1):18-32, 2019.

[72] D. H. K. Hoe et al., "Towards secure analog designs: a secure sense amplifier using memristors," Proc. *ISVLSI*, 2014.

[73] N. Hu, M. Ye, and S. Wei, "Surviving information leakage hardware Trojan attacks using hardware isolation," *IEEE Trans. Emerging Topics in Computing*, 7(2):253-261, 2019.

[74] S. Jha and S. K. Jha, "Randomization based probabilistic approach to detect Trojan circuits," Proc. *HASE*, 2008.

[75] Y. Jin et al., "Experiences in hardware Trojan design and implementation," Proc. *HOST*, 2009.

[76] Y. Jin et al., "Data secrecy protection through information flow tracking in proof-carrying hardware IP—Part I: framework fundamentals," *IEEE Trans. Info. Forensics and Sec.*, 12(10):2416-2429, 2017.

[77] V. Jyothi et al., "TAINT: tool for automated INsertion of Trojans," Proc. *ICCD*, 2017.

[78] S. Kan and J. Dworak, "Triggering Trojans in SRAM circuits with X-propagation," Proc. *DFTS*, 2014.

[79] C. Krieg et al., "A process for the detection of design-level hardware Trojans using verification methods," Proc. *HPCC*, 2014.

[80] C. Krieg et al., "Malicious LUT: a stealthy FPGA Trojan injected and triggered by the design flow," Proc. *ICCAD*, 2016

[81] C. Krieg et al., "Toggle MUX: How X-optimism can lead to malicious hardware," Proc. *DAC*, 2017.

[82] A. Kulkarni et al., "SVM-based real-time hardware Trojan detection for many-core platform," Proc. *ISQED*, 2016.

[83] N. Lesperance, S. Kulkarni, and K. T. Cheng, "Hardware Trojan detection using exhaustive testing of k-bit subspaces," Proc. *20th ASP-DAC*, 2015.

[84] H. Liu, H. Luo, and L. Wang, "Design of hardware Trojan horse based on counter," Proc. *Intl. Conf. on QRRMS Engineering*, 2011.

[85] B. Liu and R. Sandhu, "Fingerprint-based detection and diagnosis of malicious programs in hardware," *IEEE Trans. Reliability*, 64(3):1068-1077, 2015.

[86] S. Mal-Sarkar et al., "Design and validation for FPGA Trust under hardware Trojan attacks," *IEEE Trans. Multi-Scale Comp. Sys.*, 2(3):186-198, 2016.

[87] M. Muehlberghuber et al., "Red team vs. blue team hardware Trojan analysis," Proc. *HASP*, 2013.

[88] S. Narasimhan, R. S. Chakraborty, and S. Chakraborty, "Hardware IP protection during evaluation using embedded sequential Trojan," *IEEE Design & Test of Computers*, 29(3):70-79, 2012.

[89] M. Rathmair, F. Schupfer, and C. Krieg, "Applied formal methods for hardware Trojan detection," Proc. *ISCAS,* 2014.

[90] T. Reece, D. B. Limbrick, and W. H. Robinson, "Design comparison to identify malicious hardware in external intellectual property," Proc. *ICESS*, 2011.

[91] H. Salmani, "COTD: reference-free hardware Trojan detection and recovery based on controllability and observability in gate-level netlist," *IEEE Trans. Info. Forensics and Security*, 12(2):338-350, 2017.

[92] B. Schneier, "Evil maid attacks on encrypted hard drives," *Crypto-Gram Newsletter*, 2009.

[93] A. Sengupta and S. Bhadauria, "Untrusted third party digital IP cores: Power-delay trade-off driven exploration of hardware Trojan secured datapath during high level synthesis," in Proc. *Great Lakes Symp. on VLSI*, 2015.

[94] A. Sengupta, S. Bhadauria, and S. P. Mohanty, "TL-HLS: methodology for low cost hardware Trojan security aware scheduling with optimal loop unrolling factor during high level synthesis," *IEEE Trans. CAD*, 36(4):655-668, 2017.

[95] A. Sengupta and D. Roy, "Protecting IP core during architectural synthesis using HLT-based obfuscation," *Electronics Letters*, 53(13):849-851, 2017.

[96] B. Shakya et al, "Benchmarking of hardware Trojans and maliciously affected circuits," *J. HSS*, 1(1):85-102, 2017.

[97] D. M. Shila and V. Venugopal, "Design, implementation and security analysis of hardware Trojan threats in FPGA," Proc. *ICC*, 2014.

[98] O. Sinanoglu et al., "Reconciling the IC test and security dichotomy," Proc. *18th European Test Symposium*, 2013.

[99] C. Sturton et al., "Defeating UCI: building stealthy and malicious hardware," Proc. *SSP*, 2011.

[100] D. Sullivan et al., "FIGHT-Metric: functional identification of gate-level hardware trustworthiness," Proc. *DAC*, 2014.

[101] N. G. Tsoutsos et al., "Advanced techniques for designing stealthy hardware Trojans," Proc. *DAC*, 2014.

[102] N. Veeranna and B. C. Schafer, "Hardware Trojan detection in behavioral intellectual properties (IP's) using property checking techniques," *IEEE Trans. Emerging Topics in Computing*, 5(4):577-585, 2017.

[103] A. Waksman and S. Sethumadhavan, "Tamper evident microprocessors," *Proc. SSP*, 2010.

[104] A. Waksman and S. Sethumadhavan, "Silencing hardware backdoors," Proc. *SSP*, 2011.

[105] X. Wang et al., "Sequential hardware Trojan: side-channel aware design and placement," Proc. *ICCD*, 2011.

[106] X. Wang et al., "Software exploitable hardware Trojans in embedded processor," Proc. *Intl. Symp. on DFT*, 2012.

[107] X. Wang et al.,"IIPS: infrastructure IP for secure SoC design," *IEEE Trans. Computers*, 2015.

[108] S. Wei et al., "Hardware Trojan horse benchmark via optimal creation and placement of malicious circuitry," Proc. *DAC*, 2012.

[109] S. Wei et al., "Provably complete hardware Trojan detection using test point insertion," Proc. *ICCAD*, 2012.

[110] S. Wei and M. Potkonjak, "Malicious circuitry detection using fast timing characterization via test points," Proc. *HOST*, 2013.

[111] J. Zhang et al., "VeriTrust: verification for hardware trust," *IEEE Trans. CAD*, 34(7):1148-1162, 2015.

[112] E. Zhou et al., "Nonlinear Analysis for Hardware Trojan Detection," Proc. *ICSPCC*, 2015.

[113] M. Abramovici and P. Bradley, "Integrated circuit security: new threats and solutions," *CSIIRW*, no. 55, 2009.

[114] S. S. Ali et al., "Novel test-mode-only scan attack and countermeasure for compression-based scan architectures," *IEEE Trans. CAD*, 34(5):808-821, 2015.

[115] S. Amir et al., "Comparative analysis of hardware obfuscation for IP protection," Proc. *GLSVLSI*, 2017.

[116] C. Bao, D. Forte, and A. Srivastava, "On reverse engineering-based hardware Trojan detection," *IEEE Trans. CAD,* 35(1):49-57, 2016.

[117] S. Bhasin and F. Regazzoni, "A survey on hardware Trojan detection techniques," in Proc. *ISCAS*, 2015.

[118] S. Bhunia et al., "Hardware Trojan attacks: threat analysis and countermeasures," *Proc. IEEE*, 102(8):1229-1247, 2014.

[119] J. Francq and F. Frick, "Introduction to hardware Trojan detection methods," Proc. *DATE*, 2015.

[120] C. Liu et al., "Shielding heterogeneous MPSoCs from untrustworthy 3PIPs through security-driven task scheduling," *IEEE Trans. Emerging Topics in Comp.*, 2(4):461-472, 2014.

[121] P. Mishra et al., *Hardware IP security and trust*. Springer, 2017.

[122] C. Pilato et al., "Securing hardware accelerators: a new challenge for high-level synthesis," *IEEE Embedded Systems Letters*, 10(3):77-80, 2018.

[123] J. Rajendran, O. Sinanoglu, and R. Karri, "Regaining trust in VLSI design: design-for-trust techniques," *Proc. IEEE*, 102(8):1266-1282, 2014.

[124] J. Rajendran et al., "Fault analysis-based logic encryption," *IEEE Trans. Computers*, 64(2):410-424, 2015.

[125] J. Rajendran et al., "Belling the CAD: toward security-centric electronic system design," *IEEE Trans. CAD*, 34(11):1756-1769, 2015.

[126] M. Rostami et al., "Hardware security: threat models and metrics," Proc. *ICCAD,* 2013.

[127] M. Rostami et al., "A primer on hardware security: models, methods, and metrics," *Proc. IEEE*, 102(8):1283-1295, 2014.

[128] D. Saha and S. Sur-Kolay, "SoC: a real platform for IP reuse, IP infringement, and IP protection," *VLSI Design*, 2011.

[129] A. Sengupta et al., "Low cost functional obfuscation of reusable IP cores used in CE hardware through robust locking," *IEEE Trans. CAD*, 38(4):604-616, 2019.

[130] M. Tehranipoor and F. Koushanfar, "A survey of hardware Trojan taxonomy and detection," *IEEE Design & Test*, 27(1):10–25, 2010.

[131] M. Tehranipoor et al., "Trustworthy hardware: Trojan detection and design-for-trust challenges," *Computer*, *44*(7):66-74, 2011.

[132] X. Wang et al., "Detecting malicious inclusions in secure hardware: challenges and solutions," Proc. *HOST*, 2008.

[133] C. Baier and J.-P. Katoen, *Principles of model checking*. MIT Press, 2008.

[134] "The RISC-V Instruction Set Manual," https://tinyurl.com/yajxsfng.

[135] "OpenRISC 1000 Architecture Manual," https://tinyurl.com/yyvglmyt.